Fundamental Study for Digital Particle Analysis†

— Principle of Three Pixel Vector Method —

Katsunori INOUE* and Kazuo KIMURA**

Abstract

Fourier descriptor and shape factor, which are calculated from perimeter of a figure, are useful as an index for configuration of particles in the digital particle analysis of metal micro-structure and non-destructive inspection.

However, some errors are generated in the measurement of the perimeter for the region of a figure whose size is relatively small in the frame of the whole image. These errors are caused by the size and orientation of the figure, and are unavoidable in some cases with the conventional methods. A new method called the "three-pixel vector method" has been developed. The above errors can be reduced remarkably by this new method. The principle and the capability of this method, and a summary of the usual methods, are described in this report.

KEY WORDS : (Image Processing) (Digital Length Measurement) (Perimeter) (Pixel Connection) (Shape Factor)

1. Introduction

When applying modern particle analysis based on digital image processing to the automatic recognition of defects in nondestructive inspection and to the quantitative measurement of metal micro-structure in metallurgy, the shape factor is defined as an index of the configuration of the particles[1~3]. This factor can be calculated from the perimeter and area of individual particles being considered. As the particles in question are usually small in size relative to the frame of the image, noticeable errors often appear in the results of length measurement used to obtain the perimeter of the particles. These errors concern both the size and orientation of the particles, essentially because the pixels of the digital image are characteristically represented not by geometrical points, but by regular polygons (most often, regular squares) of definite size.

In this report, there is a discussion of the inevitability of the occurrence of such errors associated with the conventional methods of length measurement and propose of the new algorithm which is the key to reducing the occurrence of errors. The theory of length measurement using this algorithm is described and its advantages by comparing the effect of both the size and orientation of a simple figure, such as a regular square, on the results or perimeter measurement using this method and several other methods is demonstrated.

2. Various Methods of Digital Length Measurement and Occurrence of Error

For the sake of the simplicity in handling the problem, our discussion of error occurrence in relation to the various conventional methods of digital length measurememt will be limited to the binary image comprising the pixels of a regular square, the situation being similar for any other grey level image. Moreover, the tracking of the boundary of a figure for calculation of perimeter is done clockwise. These premises do not disturb the generality of the theory.

The hatched area in **Fig. 1(a)** represents the image of a massive object whose boundary pixels are extracted as shown in **Fig. 1(b)** and then counted to get their number. The hatched portion in Fig. 1(b) was extracted based on the 8-connection mode, in which diagonal connection is allowed in addition to vertical and horizontal connections. Using the 4-connection mode, in which only vertical and horizontal connections are allowed, the X-marked pixels in the figure should also be considered. This means that the perimeter would be 28 and 38 with the 8-connection and 4-connection modes respectively, by simply counting the number of these boundary pixels. such methods of digital length measurement will be called the "8-connection count method" and the "4-connection count method" in this report.

These methods of simply counting the number of pixels give rise to errors resulting from two causes. The first cause concerns the reduced size of a figure, for which

† Received on October 31, 1989

* Professor

** Graduate Student (Present address: Komatsu Co., Japan)

Transaction of JWRI is published by Welding Research Institute of Osaka University, Ibaraki, Osaka 567, Japan

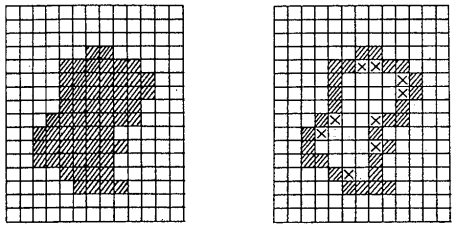

(a) Binary image (b) Boundary pixels

Fig. 1 Binary image and boundary pixels.

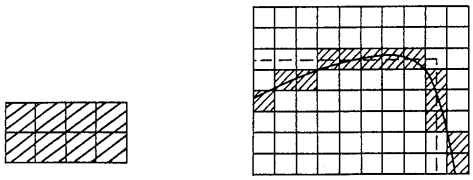

(a) In case of small rectangle (b) In case of curved line

Fig. 2 Examples of error occurence in digital length measurement.

examples are illustrated in **Fig. 2(a)** and **(b)**. For example in Fig. 2(a), the perimeter obtained by the method of counting pixels is not 12 but 8, altholugh the former is the actual value. The length of the curve represented by the solid line in Fig. 2(b) corresponds to the number of pixels represented by the hatched portion in the figure (8-connection mode), the number of which is 13. It should also correspond to the length of the broken line shown in the same figure, but the actual length of the solid line is 14 and the error is due to its small radius of curvature which is comparable to the size of a pixel. The second cause relates to the orientation of a figure. The perimeter of the square shown by way of example in **Fig. 3(a)** is 28 according to the pixel counting method, this, however, is changed to 26 by a 22.5 degree rotation of **Fig. 3(b)** when obtained by the 8-connection count method.

As is seen in these examples, if the method of length measurement does not take into account the size of the figure and changes in its orientation, errors, not to be neglected, always occur in the result. As an alternative to the simple pixel counting method, a small improvement can be made by using a method in which the pixel connection is taken as 1, in the same manner as the above-mentioned method, when pixels are connected horizontally or vertically, but counted as $\sqrt{2}$ when the connection is diagonal. The length of the curve in Fig. 2(b) is found to be $9 + 4\sqrt{2} = 14.7$ by this improved method. This method we will call the "1, $\sqrt{2}$ counting method".

An additional method may be derived from the 1, $\sqrt{2}$ counting method which improves $\sqrt{2}$ counting by substitution of $\sqrt{5}$ for the coupling of (1, $\sqrt{2}$) or ($\sqrt{2}$, 1). For the example of Fig. 2(b), the lentgth would be

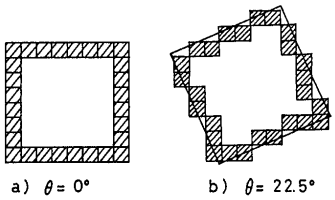

Fig. 3 Example of error occurence due to orientation of a figure.

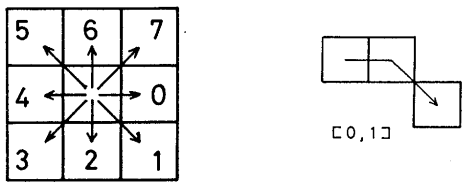

(a) Chain code table (b) An example of three-pixel chain code

Fig. 4 Chain code table and an example of three-pixel chain code.

represented by $5 + 4\sqrt{5} = 13.9$. This method we will call the "1, $\sqrt{2}$, $\sqrt{5}$ counting method". In the above two examples of the curve length measurement, only the first coupling of the pixels in the series is counted as 1 exceptionally, even if the connection is diagonal; thus the value of 1 should be deemed taking the length of a half pixel at both the start and the end points.

As will be noted later, the occurrence of error in terms of the perimeter, which is caused by change of the orientation of the figure can be suppressed appreciably by these two methods. It should be noted, however, that for the rectangle in Fig. 2(a), the perimeter would be taken as 8 even if by these two methods, just as by the simple pixel counting methods.

For this reason, the development of an accurate digital length measuring method which is characteristically less affected by both the size and the change of the orientation of the figures in an image is desirable.

3. Three-pixel Vector Method

A new algorithm for length measurement, the "three-pixel vector method", has been developed for the purpose of removing the drawbacks inherent in the conventional methods of measuring digital length. With this new method, length measurement is made with the length of the individual unit itself and the state of the connection between two adjacent basic units comprising three consecutive pixels.

The state of connection between two adjacent pixels is first expressed in terms of the chain code[4], which is well known and often used, as shown in **Fig. 4(a)**. Every group of three adjacent pixels, which is a basic unit of this method as described above, can be expressed in terms of

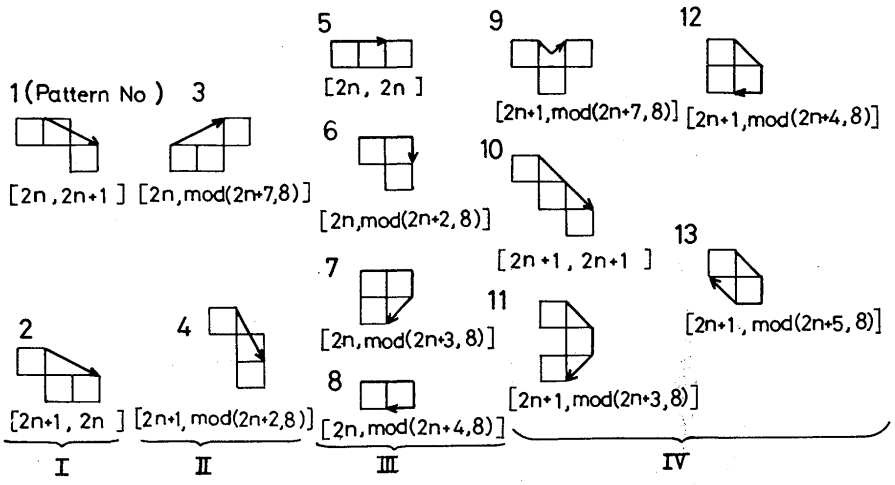

Fig. 5 13 categories of three-pixel vectors.

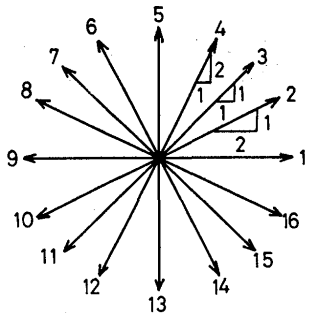

Fig. 6 Direction code.

$[k, l]$ as determined by the combination of two chain codes k and l. For example, it can be expressed by [0, 1] as shown in **Fig. 4(b)**. This expression is termed the "three-pixel chain code", for which a total of $8 \times 8 = 64$ kinds are conceivable, of which 12 kinds (3 patterns of the basic unit) should be excluded from consideration for the reason that they do not exist in clockwise boundary tracking. These three patterns are:

$[2n, \mathrm{mod}\,(2n+5, 8)]$, $[2n, \mathrm{mod}\,(2n+6, 8)]$,
$[2n+1, \mathrm{mod}\,(2n+6, 8)]$

Where $n=0-3$ and mod (l, m) denotes the remainder of the division of l by m.

The other 13 patterns of the basic unit ($13 \times 4 = 52$ kinds) are classified into 4 groups as shown in **Fig. 5**. The re-entrant figures can be considered by these patterns. In the case of counter-clockwise boundary tracking, we may use their mirror-image patterns. In the classification shown in Fig. 5, the patterns which can be denoted $\sqrt{5}$ by the 1, $\sqrt{2}$, $\sqrt{5}$ counting method are selected and termed the $\sqrt{5}$ type: then the patterns among the $\sqrt{5}$ type whose three-pixel chain code can be expressed without use of mod( ) and the other $\sqrt{5}$ type patterns are divided into Groups No.1 and No.2 respectively. Note that these two groups correspond to the case of a direction code (decribed later) of $4(4-n)$ and $\mathrm{mod}(18-4n, 16)$ (or $\mathrm{mod}(14-4n, 16)$) respectively. Otherwise, the patterns belong to Groups No.3 or No.4, depending on whether the first element of the three-pixel chain code of the basic unit is an even number or odd number.

Then, the length of the basic contour line, indicated by the arrow in Fig. 5, is assigned to each pattern of four groups and is defined as 1, which can be expressed by Eq. (1) as a vector.

$$\boldsymbol{l}_b=(l_{bi})=(\sqrt{5}, \sqrt{5}, \sqrt{5}, \sqrt{5}, 2, 3, 3+\sqrt{2}, 4, \sqrt{2}, 2\sqrt{2}, 1+2\sqrt{2}, 2+\sqrt{2}, 2+2\sqrt{2})^{\mathrm{T}} \quad (1)$$

Where l_{bi} is a basic contour of i-th pattern and T stands for transposition. The basic contour is represented by 1 to 3 sections of line; the directions, one start and the other end, being expressed in terms of the direction code as illustrated in **Fig. 6**, the matrix $\boldsymbol{D}$ for the 13 patterns is given by

$$\boldsymbol{D}=(D_{i,j})=\begin{pmatrix} 4(4-n), & 4(4-n), & f(18), & f(14), & f(17), \\ 4(4-n), & 4(4-n), & f(18), & f(14), & f(17), \end{pmatrix}$$
$$\begin{matrix} f(17), & f(17), & f(17), & 15-4n, & 15-4n, \\ 13-4n, & f(27), & f(25), & f(19), & 15-4n, \\ 15-4n, & 15-4n, & 15-4n & & \\ f(27), & f(25), & f(23) & & \end{matrix} \quad (2)$$

Where $f(N) \equiv \mathrm{mod}(N-4n, 16)$, $D_{i,1}$ and $D_{i,2}$ express the directions of start and end respectively and i corresponds to one of the 13 patterns of Fig. 5. Each pattern belongs to Group No.1 or 2 or 3 or 4 depeding on wheter i is equal to 1,2 or 3,4 or 5−8 or 9−13 respectively.

Next, the concept of the connection between the adjacent basic units is introduced The last pixel of the preceding basic unit overlaps with the top pixel of the succeeding basic unit, forming a basic unit coupling; this means that

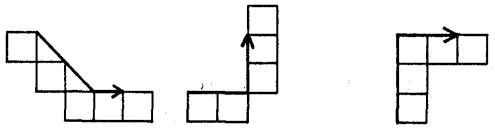

Fig. 7 Examples of three-pixel connection.

the pixels of five series are involved in this coupling. A total of 2704 unit coupling combinations are conceivable according to the concept introduced, of which 1104 combinations cannot exist in clockwise boundary tracking and remaining 1600 actually existing.

For all of these actually existing combinations, the effective length of the basic unit coupling is found by the following calculation. A change in the relative direction between both $(N-1)$th and Nth basic units as counted from the starting point of the measurement is first calculated by Eq. (3),

$$\Delta^{N}D = \mathrm{mod}\,[\,({}^{N}D_{k,1} - {}^{N-1}D_{1,2} + 16),\ 16] + 1 \quad (3)$$

Where ${}^{M}D_{m,n}$ on the right side of the equation indicates the direction code of the Mth basic unit to be the m, n element in matrix $\boldsymbol{D}$ of Eq. (2).

Then, an adjustment is made to the original length of the basic unit coupling, which is the sum of the basic contour line length of two units, in respect of the value of the direction change $\Delta^{N}D$. The matrix designed for this adjustment is as represented by Eq. (4),

$$\boldsymbol{\Delta l} = (\Delta l_{i,j}) = \begin{pmatrix} 0, & 0, & 0, & 0, & \sqrt{2}-\sqrt{5}, \\ 0, & 0, & \sqrt{2}-\sqrt{5}, & \sqrt{2}-\sqrt{5}, & \sqrt{2}-\sqrt{5}, \\ 0, & -1, & -1, & 2-\sqrt{5} & 0, \\ 0, & 0, & 0, & \sqrt{2}-\sqrt{5}, & \sqrt{5}-2\sqrt{2}, \end{pmatrix}$$

$$\begin{pmatrix} 1-\sqrt{2}, & 2-\sqrt{5}, & 0, & 2, & 2, & 2, & 2, & 1, & 1, & 1, & 1 \\ 0, & & 0, & 2, & 2, & 2, & 1, & 1, & 1, & 1, & 0, & 0 \\ 0, & & 0, & 0, & 2, & 1, & 1, & 1, & 1, & 0, & 0, & 0 \\ 2-\sqrt{5}, & & 0, & 2, & 2, & 2, & 2, & 1, & 1, & 1, & 1, & 0 \end{pmatrix} \quad (4)$$

All the elements in the above matrix were obtained by the careful examination of 1600 individual combinations; the individual rows i correspond to Groups No.1−No.4 to which the pattern of the Nth basic unit belongs and the individual columns j correspond to the value of change $\Delta^{N}D$ in direction found by Eq. (3). For example, if we consider **Fig. 7(a)**, **(b)** and **(c)**, to represent the connection of the $(N-1)$th and Nth basic units, in Fig. 7(a), the direction code of the $(N-1)$th basic unit is ${}^{N-1}D_{10,2}=15$ as n=0, i=10, and that of the Nth basic unit is ${}^{N}D_{5,1}=15$ as n=0, i=5; from Eq. (3), $\Delta^{N}D=\mathrm{mod}(2,\ 16)+1=3$, then the ajdustmant Δl becomes the (3, 3) element $l_{3,3}$ (= −1) of the matrix in Eq. (4) from the value of $\Delta^{N}D$ and the fact that the Nth basic unit belongs to Group No.3 as i = 5. Then, the perimeter P of five pixel connection indicated by the arrow in Fig. 7(a) amounts to $2\sqrt{2}+1$. Similarly, in Fig. 7(b), we have $D=\mathrm{mod}(5-2+16,16)+1=4$, $\Delta^{N}l=\Delta l_{3,4}=2-\sqrt{5}$, $P=\sqrt{5}+2+2-\sqrt{5}=4$, and in Fig. 7(c), $\Delta^{N}D=\mathrm{mod}(1-5+16,\ 16)+1=13$, $\Delta^{N}l=\Delta l_{3,13}=1$, $P=2+2+1=5$.

According to the principle described above, any perimeter P_n extending from the starting point to the Nth basic unit can then be calculated using Eq. (5),

$$\begin{cases} P_n = P_{n-1} + {}^{N}l_b + \Delta^{N}l \ (n > 1) \\ P_1 = {}^{1}l_b \end{cases} \quad (5)$$

When a line to be measured for its length is a closed curve and the number of the composing pixels is even or an open curve and the number is odd, this principle is applicable to all the basic units between the starting and the ending point (in the closed curve, the same point). In cases where the number is odd for a closed curve or even for an open curve, the same principle can be applied to all the units except the terminal portion of the tracked cruve, to which only the 1, $\sqrt{2}$ counting method should be applied.

4. Comparison of Various Methods of Perimeter Measurement

4.1 Image input and evaluation of the result of perimeter measurement

The various methods of measuring the perimeter were applied to an actual figure to compare perimeter measuring characteristics. Both generation of a figure and length measurement can be accomplished by computer simulation, but we input a digital image and processed it, using a TV camera, image pick-up and processing device, to make the measurement more practical in this research. The latter method incorporates, to a certain degree, the effect of possible distortion or noise on the image input.

The input image was black on a white background at a high level of contrast, contributing greatly to the ease with which the binarization of the figure image could be made. The input figure was regular square, one of the simplest geometric shapes. The accuracy of the applied method of length measurement was evaluated by the shape factor calculated in Eq. (6)[5].

$$K = P^2/4\pi S \quad (6)$$

where S denotes the area of the figure found by counting the number of its internal pixels and P is the perimeter as a target for measurement, which is theoretically $4/\pi$ ($\equiv K_0$) for a regular square figure. For comparison, the value K was calculated for the input figure and then relative error E was calculated from Eq. (7) for various

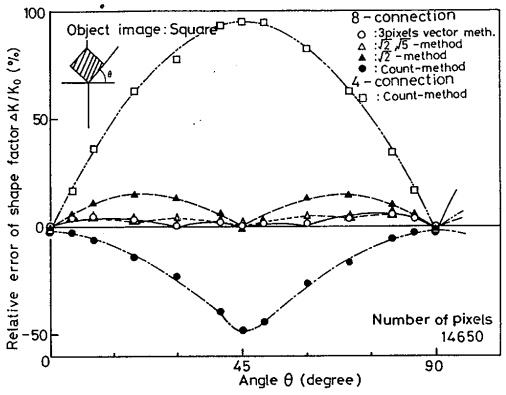

Fig. 8 Relative errors of shape factor due to orientation of a figure calculated by several kinds of digital length measuring methods.

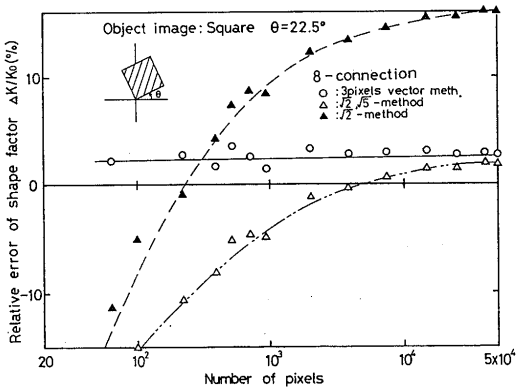

Fig. 9 Relative errors of shape factor due to size of a figure found calculated by several kinds of digital length measuring method.

length measurement methods.

$$E=(K-K_0)/K_0=\Delta K/K_0 \qquad (7)$$

Image processing was done with an ordinary system. The program was coded in SVS-FORTRAN[6] for use with a 68K CP/M operating system. The SPIDER[7] subroutine package for image processing was also used when needed.

4.2 Perimeter measurement by various methods and comparison of the results suring the shape factor

For the measurement of the perimeter P in Eq. (6) by the various methods, the input image was first binarized at a suitabale threshould level. The pixels existing in the boundary were then extracted and their coordinates found using the 4- or 8-connection mode boundary tracking algorithm. The value of S was found by counting the number of the boundary and inner pixels in both modes. The total number of boundary pixels was taken as the perimeter P in the 4- and 8-connection pixel counting methods. Next came the conversion of the connections of these pixels, considering their coordinates, into the chain code shown in Fig. 4(a). The SPIDER subroutine package was used for these two concecutive processings. The value of P was found in the 1, $\sqrt{2}$ counting method by multiplying by $\sqrt{2}$ the number of extracted pixels if their chain code was an odd number.

The value of P in the 1, $\sqrt{2}$, $\sqrt{5}$ counting method, the length of the basic contour lines stated in Eq. (1) and the direction code contained in Eq. (2) were obtained by conversion of the chain code series into the three-pixel chain code series, followed by the two-dimensional list processing. The values of the direction change were found from Eq. (3) and the adjustment values were found in the two dimensional list which corresponds to Eq. (4) by the values of the direction change and the group number of the basic units classified according to the three-pixel chain code. The value of P by the three-pixel vector method was then obtained by using the adjustment values thus calculated and Eq. (5).

The relative error of the shape factor calculated from Eq. (7) using the values of P obtained by each of the above-mentioned methods is shown in **Figs. 8** and **9** for comparison. Figure 8 shows the orientation dependence of the error, where very large errors occur, especially for both the 4- and 8-connection simple pixel counting methods. Figure 9 is a comparison of the effect of figure size on the 1, $\sqrt{2}$ counting method and the 1, $\sqrt{2}$, $\sqrt{5}$ counting method, which are less affected by the orientation of the figures, and the three-pixel vector method. It clearly demonstrates that the smaller the figure size and the fewer its inner pixels, the larger the error becomes with both types of conventional counting method. Theoretically speaking, Equation (6) gives the minimum value of the shape factor as the value of K for a circular figure, and the value of K must be greater than 1 for all types of figure. Notwithstanding this, it was confirmed by the experiment that when the number of pixels was small, the shape factor K dropped below 1 for both types of conventional counting method. This menas ingression into the "Sanctuary" due to error of measurement.

On the other hand, it should be noted that the three-pixel vector method was hardly affected by the size or orientation of the figure, and its relative error of shape factor suffered ingression.

5. Conclusion

The three-pixel vector method has been demonstrated superior to any other conventional method for finding the perimeter of a digital image to determine the shape factor and other values. It will be found to offer very useful means not only for computerized recognition of weld defects in non-destructive inspection, but also for particle

analysis of metal micro-structure and biotissue, etc.

References

1) Rosenfeld, A., Kak, A. C. 'Digital picture processing' Academic Press (1976)
2) Gonzalez, R. C., Wintz, P. 'Digital image processing' Addison-Wesley (1977)
3) Hall, E. L. 'Computer image processing and recognition' Academic Press (1979)
4) Freeman, H. 'On the encoding of arbitrarly geometric configuration' IRE Trans., EC-10 (1961) pp260-268
5) Stenson, H. H. 'The physical factor structure of random forms and their judged complexity' Perception & Psychophysics 1 (1966) pp303
6) Bath, J., Granville. R. S., McGilton. H. 'FORTRAN reference manual' Silicon Publication (1983)
7) Denshigijyutsu Sogo Kenkyusho (ETL) 'Gazoshori Subroutine Package SPIDER User's Manual' (1980)
8) Ohtsu, N. 'Discriminant and least square threshould selection' 4IJCPR (1978) pp592-596